CHF Simulation using a Non-Heating Experimental Method

Hae-Kyun Park and Bum-Jin Chung[*]
Department of Nuclear Engineering, Kyung Hee University
#1732 Deogyeong-daero, Giheung-gu, Yongin-si, Gyeonggi-do, 17104, Korea
[*]*Corresponding author*: bjchung@khu.ac.kr

1. Introduction

The boiling heat transfer accompanies vigorous heat transfer rates compared to the single phase heat transfer. Hence, many of engineering devices have been operated in boiling regime. However, when unexpected excess temperature is reached at the heat transfer surface, the film boiling will occur at a certain condition and it may cause failure of the system [1]. This phenomenon is termed as CHF and it is one of the prime issue of the nuclear industry, which utilizes high heat flux from the fission reactions. Thus, CHF can be a crucial parameter in the design criterion at the nuclear system. Although many researchers [2-8] have been studied for CHF during several decades, the phenomenological interpretation is not clarified so far and it is not easy to achieve and observe CHF condition due to the highly excess temperature.

In this paper, the authors propose the non-heating experimental methodology in order to simulate CHF situation, which is hard to establish because of its harsh condition through the heat transfer experiment. The authors employed sulfuric solution copper electroplating system, which generates hydrogen vapor at the surface. When potential is applied, the hydrogen ions dissolved in the solution reduce at the cathode surface as current flows. In order to verify our newly introduced methodology, the measured Critical Mass Flux (CMF) and observation results were compared with CHF results of the previous heat transfer studies.

2. Existing studies

Many researchers have been studied for CHF phenomena of pool boiling conditions experimentally and analytically. Here are some CHF models, which have been widely accepted.

2.1 Hydrodynamic Instability Model

Kutateladze [2] proposed CHF predicted correlation based on a dimensional analysis in an earlier study. Before long, Zuber [3] established hydrodynamic instability model, which have been widely accepted. Zuber developed Kutateladze's CHF correlation applying to the Rayleigh-Taylor instability as expressed in Eq. (1). In this case, diameter of the vapor columns were assumed a half of Rayleigh-Taylor wavelength. At CHF condition, vapor velocity assumed by Kelvin-Helmholtz instability. Compared with the existing experimental data, *K* value was determined as 0.131.

$$q''_{CHF} = K h_{lg} \rho_g^{1/2} [\sigma g (\rho_l - \rho_g)]^{1/4} \tag{1}$$

2.2 Macrolayer Dryout Model

Haramura and Katto [4] postulated the macrolayer dryout model. They improved Katto and Yokoya's study [5] and insisted that the heat transfer at a certain high heat flux is related with presence of macrolayer. Macrolayer is located underneath of the vapor mushroom, which can be observed in the nucleate boiling regime at a high heat flux. It is composed of vapor stems and thin liquid layer. Thus, the CHF occurs when the liquid layer is completely evaporated during hovering time, which is a period from generation to departure of the vapor mushroom. And they postulated thickness of the macrolayer as a forth of Kelvin-Helmholtz wavelength. Hence, CHF predicted correlation from the heat balance equation can be derived in terms of the liquid vaporization in the macrolayer.

$$\tau_d q''_{CHF} = \delta_l h_{lg} \rho_l (A_h - A_v) \tag{2}$$

τ_d, δ_l, A_h and A_v is hovering period, thickness of macrolayer, heated area, and area of the vapor stem respectively. Thus, Eq. (3) can be derived introducing Eq. (2).

$$q''_{CHF} = h_{lg} \rho_g^{0.5} [\sigma g (\rho_l - \rho_g)]^{1/4} (1+k)^{5/16} \left(\frac{\pi^4}{2^{11} \cdot 3^2}\right)^{1/16} \tag{3}$$

$$\left(\frac{A_v}{A_w}\right)^{5/8} \left(1 - \frac{A_v}{A_w}\right)^{5/16} \left[\left(\frac{\rho_l}{\rho_g}+1\right) / \left(\frac{11}{16}\frac{\rho_l}{\rho_g}+1\right)^{3/5}\right]^{5/16}.$$

2.3 Other Models

Kandlikar [6] interpreted the CHF phenomena theoretically in terms of vapor bubble receding contact angle. It means that receding contact angle between heater surface and vapor bubble may effect of the CHF. Kandlikar suggested CHF correlation, which is well agreed with Kutateladze's correlation and existing experimental results. However, Kandlikar's model predicted well rather than Kutateladze's model for the vertical plates. Because the suggested correlation considers both hydrodynamic effect and non-hydrodynamic effect such as receding contact angle and orientation of the heater.

As high speed camera recording technology advanced, the researchers could observe and analyze CHF phenomena in high quality [7-8]. Ahn and Kim [7] showed presence of macrolayer and dry patch in the vicinity of the CHF using high speed camera. They employed diameter of 10 mm upward facing copper disk

as a heater. In this case, CHF was increased due to inflow at the edge of the heater. Because the inflow interrupted vaporization process at the macrolayer. For the same reason, the macrolayer forms as a concave shape.

3. Experiments

3.1 Methodology

The copper electroplating system was introduced in order to simulate CHF phenomenon. The system is composed of anode and cathode electrodes submerged in a solution of sulfuric acid. As the applied potential between anode and cathode increases, the current increases resulting in the evolution of hydrogen gas. This phenomenon is similar to that of the vapor production in the heat transfer system.

The basic idea of this study is that the CHF phenomenon due to the departure of nucleate boiling and film boiling by the generation of the vapor can be simulated through the hydrogen gas generation in mass transfer system. If hydrogen gas generation exceeds a certain limit, hydrogen film can be made. Although it is strictly differ from the two-phase flow to the two-component flow in terms of the chemical identity, there are several points of similarity between two of them: general phenomenon, analysis and experimental method [9].

In the two phase flow, hydraulic behaviors of vapor over the arbitrary solid surface will be similar to the two-component flow under the identical gaseous volume condition. Hence, the volume generation rate of the hydrogen can be calculated with Eq. (4) and it can be transformed to the corresponding heat flux using Eq. (5).

$$\eta = V_R \left(\frac{T}{273.15} \right) \left(\frac{I_{CMF}}{neN_A} \right) \qquad (4)$$

Volume generation rate of the hydrogen in the present work (m³/s), η can be calculated by the applied current, I over products between n, e and N_A, which represent number of the electron charge to reduction hydrogen ion, magnitude of the charge of an electron and Avogadro constant, respectively. And the volume per unit mole of the gaseous (m³/mole), V_R transforms molar generation of hydrogen into volume generation, which was dependent on the temperature regarding to the Charles's law. And then the applied heat flux is simulated as follows

$$q_{CHF} = \eta h_{fg} \rho_g \qquad (5)$$

The products of calculated η in Eq. (4) by present experiment, latent heat, h_{fg} and density of vapor, ρ_g transforms the applied current at CMF condition into the CHF condition in the heat transfer system.

3.2 Experimental Apparatus

The experimental apparatus and electric circuit are shown in Fig. 1. A 10 mm diameter of horizontal upward facing copper disk was located in a top-opened reservoir. This cathode disk simulates heated surface. And an anode copper plate of 0.01 m × 0.05 m is placed against the cathode to supply electric charges. The power supply (SGI 100A/150V, SGI) was used for potential control and Data Acquisition system (34972A, Agilent) was used for recording the data.
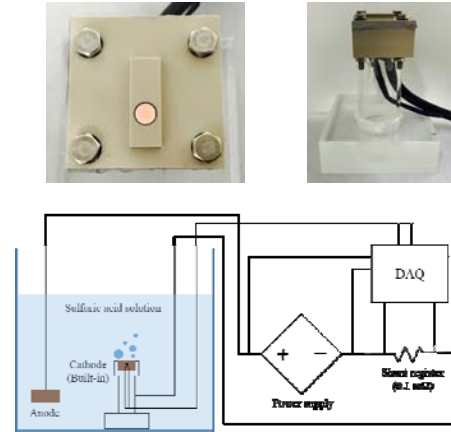
Fig. 1. Photographs of the test apparatus and electric circuit.

4. Results and discussion

4.1 CMF measurement

Figure 2 shows the measured current (I) and potential (V) during experiment. Current increased as applied potential increased at low-current region, which is similar to the nucleate boiling region of the conventional boiling curve. When current density exceeded about 317.80 kA/m², a sudden drop was measured. It seems that the coalescence of hydrogen mushroom on the cathode plate blocked supplement of the electron charge. So that the CMF was measured at 317.80 kA/m². And this CMF can be transformed to CHF by using Eq. (4) and (5), 60.42 kW/m². This result is about 25 times smaller than that of the heat transfer results by Haramura and Katto's [4] and Ahn and Kim's [7] experiments, which were conducted identical geometry condition with present works.
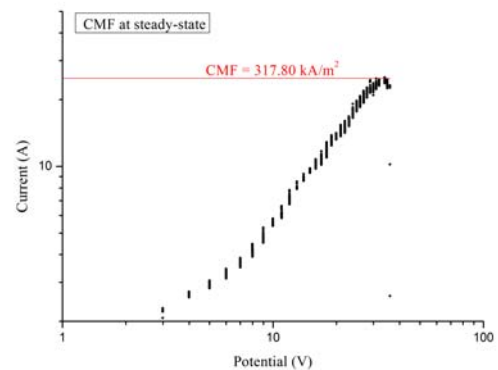
Fig. 2. CMF result using mass transfer system.

4.2 Departure hydrogen diameters

Table 1 lists departure bubble diameters of the hydrogen bubble at low current regime (Under 851.80 A/m^2). The high speed camera (Phantom, v7.3-4GB Mono) was used for still cuts of the departure bubble, which was not coalesced and departed independently. The average hydrogen departure diameter was 0.124 mm. The resolution of the image was 7.47 μm. However, the typical range of departure bubble diameters measured by various researchers in heat transfer system using water under 0.1 MPa were from 2 mm to 3 mm [10]. Thus, the departure hydrogen diameter is about 20 times smaller than those of the heat transfer results. The solid surface-to-gaseous interaction such as surface tension or certain electro-chemical reaction may cause these discrepancy.

Table 1. Departure hydrogen diameters.

1st trial	
Average current (A)	**Hydrogen diameter (mm)**
0.0098	0.15647
	0.12713
0.0119	0.13691
	0.16625
0.0124	0.08801
	0.11735
	0.14669
	0.12713
	0.11735
	0.09779
	0.11735
0.0131	0.08801
	0.13691
	0.16625
2nd trial	
Average current (A)	**Hydrogen diameter (mm)**
0.0189	0.15653
	0.09208
	0.12891
0.0174	0.10128
	0.08287
	0.12891
0.0669	0.11970
	0.11049
	0.12891
Average Hydrogen diameter = 0.124 mm	

4.3 Behaviors of hydrogen film

Figures 3 and 4 compare the hydrogen and vapor film [7] just after the CMF and CHF value. The average current density at the Fig. 3 was measured at 71.17 kA/m^2. The mushroom hovering period was about 180 ms, which was about 2 or 3 times larger than that of Ahn and Kim [7], Katto and Yokoya's results [5] in heat transfer experiments. There are some difficult points were observed that the generation process of the second mushroom between this work and Ahn and Kim's results [7]. In present work, the first mushroom departs and second bubbles underneath of the first mushroom coalesces. However, these second bubbles that can be observed Fig. 3(b)-(d) were much smaller than that of the first mushroom. Meanwhile, the only single clot of the second bubble can be observed at Ahn and Kim's result.

(a) 0 ms   (b) 30 ms   (c) 60 ms

(d) 90 ms   (e) 120 ms   (f) 150 ms

(g) 180 ms
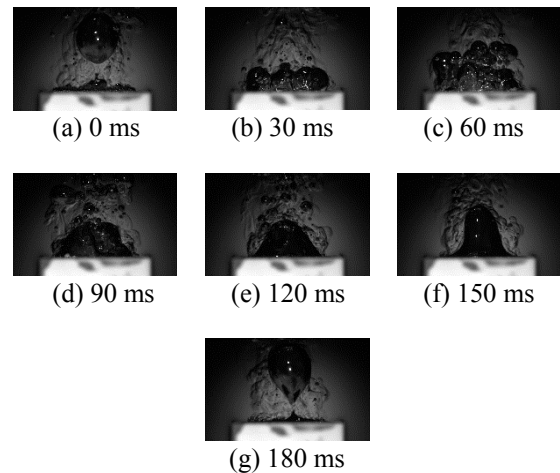
Fig. 3. Photographs just after CMF.
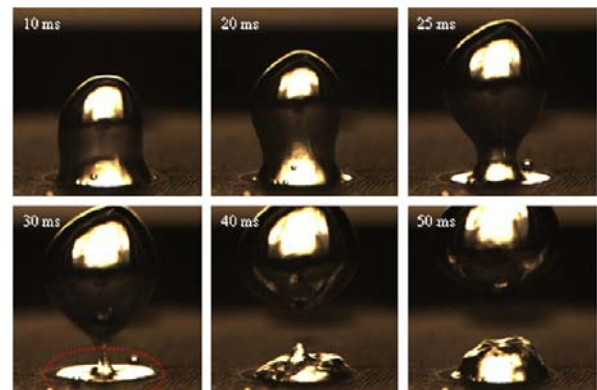
After CHF, entire vapor film boiling

Fig. 4. Photographs just after CHF [7].

5. Conclusion

CHF phenomena is simulated by hydrogen gas using copper electroplating system. Vapor behavior on present work experiment was visualized using high speed camera, and it was similar to that of on the heat transfer.

CMF value was measured by hydrogen gas with high current value. Thus, this measured CMF value was transformed to the CHF value using isovolumetric concept. However, the transformed CHF from this work was 25 times smaller than that of the previous heat transfer results with identical geometry condition.

The departure bubble diameters of hydrogen were measured. The average departure hydrogen bubble diameter was 0.124 mm. Meanwhile, previous heat transfer results for water were from 2 mm to 3 mm. The authors insisted that the certain interaction between solid surface-to-hydrogen gas such as electro-chemical reaction may cause this results. The further works will conduct in this perspective.

The mushroom hovering period and succession process of present work were slightly different with those of the heat transfer system. The authors also suspect that this result was dependent on small departure bubble diameter of hydrogen.

It is concluded that consideration for these discrepancies need additional parametric analysis: two phase and two component system, surface wettability, electro-chemical reaction, etc.

ACKNOWLEDGMENT

REFERENCES

[1] F. P. Incropera, Foundation of Heat Transfer, John Wiley & Sons, New Yotk, pp. 622-638, 2012.
[2] S. S. Kutateladze, A hydrodynamic model of the critical heat transfer in boiling liquids with free convection, Zhurn. Tekhc., Fiz., Vol.20, pp. 1389-1392, 1950.
[3] N. Zuber, Hydrodynamic aspects of boiling heat transfer, AEC Report No. AECU-4439, Physics and Mathematics, 1959.
[4] Y. Haramura and Y. Katto, A new hydrodynamic model of critical heat flux, applicable widely to both pool and forced convective boiling on submerged bodies in saturated liquids, International Journal of Heat and Mass Transfer, Vol.26, pp. 389-399, 1983.
[5] Y. Katto and S. Yokoya, Principal mechanism of boiling crisis in pool boiling, International Journal of Heat and Mass Transfer, Vol.11, pp. 993-1002, 1968.
[6] S. G. Kandlikar, A theoretical model to predict pool boiling CHF incorporating effects of contact angle and orientation, Journal of Heat Transfer, Vol.123, pp. 1071-1079, 2001.
[7] H. S. Ahn, M. H. Kim, Visualization study of critical heat flux mechanism on a small and horizontal copper heater, International Journal of Multiphase Flow, Vol.41, pp. 1-12, 2012.
[8] I. C. Bang, S. H. Chang, W. P. Beak, Visualization of a principle mechanism of critical heat flux in pool boiling, International Journal of Heat and Mass Trasnfer, Vol.48, pp. 5371-5385, 2005.
[9] G. B. Wallis, One-dimensional two-phase flow, McGraw-Hill, 1969.
[10] N. I. Kolev, Multiphase Flow Dynamics 2, Springer Berlin Heidelberg, pp. 417-438, 2007.